Thin Solid Films 711 (2020) 138272

Contents lists available at ScienceDirect

Thin Solid Films

journal homepage: www.elsevier.com/locate/tsf

Robust transparent conducting electrode based on silver nanowire coating on polyelectrolytes multilayers

Jedsada Chavalitkul[a], Olivier Margeat[b], Jörg Ackermann[b], Stephan T. Dubas[a,*]

[a] Petroleum and petrochemical college, Chulalongkorn university, Bangkok, 10330, Thailand
[b] Aix Marseille Univ, CNRS, CINaM, Marseille, France

ARTICLE INFO

Keywords:
Transparent flexible electrode
Silver nanowires
Polyelectrolyte multilayers
Peeling test
Poly(ethylene terephthalate)

ABSTRACT

Transparent conductive electrodes were fabricated by the deposition of silver nanowires (AgNW) on various substrates modified by the deposition of polyelectrolyte multilayers (PEM) as primer. The PEM primer films were coated on the glass substrate by the sequential deposition of 7 or 8 layers of poly(diallyl dimethyl ammonium chloride) (PDADMAC) and poly(styrene sulfonate) to improve the adhesion of AgNW and produce flexible transparent conducting electrode. AgNW, with a diameter of 20–30 nm and 10–30 μm in length, were synthesized using a modified solvothermal method using glycerol and poly(vinyl pyrrolidone) as reducing and capping agent. The physicochemical properties of the AgNW coated PEM were characterized using UV–Vis spectroscopy, atomic force microscope and field emission scanning electron microscope. The electrical conductivity of the layer was measured by 4 points probe and a standard scotch tape peeling test was used to investigate the stability of the coated AgNW on the PEM. The PEM 7 layers (with PDADMAC as outer layer) gave the best results to immobilize AgNW with the lowest sheet resistance (14 Ω/square) while maintaining excellent transparency (85% transmission at 550 nm) even after up to 6 peeling test cycles. Finally, to demonstrate the benefit of this method, poly(ethylene terephthalate) sheet was coated with PEM primer and AgNW to produce flexible transparent conducting electrode.

1. Introduction

Transparent conductive electrodes (TCE) are needed in electronic devices such as organic light emitting diodes [1], solar cell [2–6], liquid crystal displays [7,8] as back electrode that allows light transmission either in or out of the cell. Typically, TCE are fabricated by the deposition of indium tin oxide (ITO) on a glass substrate which provides good transparency (90%) in the visible range with an excellent conductivity (13 Ω/square) [9,10]. Because the ITO coatings are still expensive, alternative materials have been proposed to replace the ITO such as metal nanowires [11–14], carbon nanotube [15,16] or graphene [17], as well as composite hybrid materials of silver nanowire (AgNW) with ITO [18], poly(3,4-ethylenedioxythiophene):poly(styrene sulfonate) [19,20] and zinc oxide (ZnO) nanoparticles [21–24]. Silver nanoparticles and more precisely AgNW are often described as one of the most promising alternatives due to excellent electrical conductivity and high transparency [25]. For the development of electrodes used in photo-voltaic devices such as solar cells or light emitting diodes, a transparency of at least 85% and a sheet resistance of less than 15 Ω/square is needed to compete with commercial ITO. These wires are usually synthesized using the polyol process with ethylene glycol as reducing agent and poly(vinylpyrrolidone) (PVP) as stabilizer [26,27]. In this research, PVP is used as a stabilizer as well as growth enhancer through preferential adsorption on Ag facets leading to the unidirectional growth of the wire. Several parameters are known to affect the AgNW growth such as PVP molecular weight [28,29], reaction temperature [29,30], and reaction time [29,30]. Once synthesized, the AgNW can be deposited on a flat substrate by spin coating [31,32], spray coating [33–36], or drop and rod casting [37,38] yet the stability of the wire on the substrate largely depends on the types of interaction with the substrate. In Table 1, the electrical and optical performance of previously published work for different coating methods and substrates are reported. It is clear that drop cast [37] and spray coating [33–36] provide good transparency and conductivity yet, no report of peeling resistance has been made. The only reference to peeling test is on Youngsang et al. [32] but it involves the spin coating of AgNW later transferred to a polymer layer which requires further silver nitrate and glucose treatment to fuse the nanowires together and obtain a peeling resistant coating. The peeling test is thought to be critical as it reflect the stability of the nanowires onto a substrate during the various

* Corresponding author.
E-mail address: Stephan.d@chula.ac.th (S.T. Dubas).

https://doi.org/10.1016/j.tsf.2020.138272
Received 3 January 2020; Received in revised form 7 July 2020; Accepted 7 August 2020
Available online 07 August 2020

Table 1
Comparison of the TCE fabricated using different deposition methods.

Deposition method	Resistance (Ω/square)	%T	Bending test (Cycles)	Peeling test (Cycles)	Type of substrate	Ref.
Spin coating	54	92	–	–	PET	[31]
Peel transferred	54	92	10,000	100	PET	[32]
Drop cast	80.6	9.3	–	–	PET	[37]
Spray coating	90	86	10,000	–	PET	[33]
Spray coating	19	81	–	–	Glass	[34]
Spray coating	10	80	–	–	Glass	[35]
Spray coating	100	98	–	–	PC	[36]
Meyer rod	12.1	71	–	–	PC	[38]
Meyer rod	24	91	–	–	PET	[39]
Dip coating	10	58	1000	–	Glass	[40]
Hot pressed	12	83	800	–	Glass	[41]
This work	**14**	**85**	**1000**	**6**	**Glass**	

processing steps needed during the fabrication of any photo-voltaic device. In case of poor adhesion, the loss of AgNW might lead to a loss of performance of the device.

Polyelectrolyte multilayer (PEM) thin films fabricated using the so called layer-by-layer deposition can be used to modify the surface of glass or poly(ethylene terephthalate) (PET) through the electrostatic or Van der Waals interactions [42,43]. The polyelectrolytes adhere onto the substrate through electrostatic interaction and in some case through weak Van der Waals interaction. These versatile and easy to process technique are applicable to large scale samples and environmental friendly. Since the PEM coatings are transparent ultrathin film of few tens of nanometers, they can be used as a primer to immobilize AgNW on any given substrate. Publications describing the deposition of AgNW on PEM because polyelectrolytes are generally electrical insulator which affect the electrical conductivity of AgNW thin film. Previously, PEM coating based on the assembly of poly(allylamine hydrochloride) (PAH) and AgNW were achieved by dip coating to get films with a sheet resistance of 60 Ω/square and a transparency of 78% transmission. The sheet resistance was relatively high compared to the commercial ITO coated on the glass which is around 13.6 Ω/square. The lower conductivity is probably due to the insulating PAH coating in between each AgNW layers which acts as insulating barrier [40]. A more efficient approach to improve the conductivity is possibly to limit the AgNW coating to a single layer on top of a PEM, which is used to anchor and stabilize the wires. If successful, a standard peeling test should be used to confirm the anchoring and stability of the silver wires on the PEM substrate while maintaining good transparency and good conductivity.

In this paper, robust transparent conducting electrodes were prepared by spin coating of PVP stabilized AgNW on a PEM primer layer coated on a glass substrate. To investigate the effect of the top layer charge, PEM composed of 7 (positively charged on top) or 8 layers (negatively charged on top) were used as adhesive layer to anchor the AgNW. The conductivity and transparency of the different coating was compared using 4-points probe measurements before and after up to 6 peeling test cycles. Finally, the AgNW were also deposited on a PET substrate to fabricate flexible TCE, to be used in flexible solar cell application.

2. Experimental

2.1. Material

Silver nitrate ($AgNO_3$, ACS reagent, >99.0%), glycerol (>99.5%), poly(diallyl dimethyl ammonium chloride) solution (PDADMAC, medium molecular weight, 20 wt.% in H_2O, MW 200,000–350,000), poly(sodium 4-styrenesulfonic acid) sodium salt (PSS, average MW 70,000), sodium chloride (NaCl, ACS reagent, >99.0%) were purchased from Sigma-Aldrich. Poly(vinylpyrrolidone) (PVP, M.W. 1,300,000) was purchased from Alfa Aesar. Absolute ethanol (EMPROVE®) were purchased from Merck. All chemicals were analytical grade and used without further purification.

2.2. Synthesis of AgNW

The AgNW were synthesized using a modified solvothermal method in which ultra-long silver nanowires of over 20 μm could be produced [44]. In this method 2.553 g of PVP were dissolved in 70 mL of glycerol under stirring at 100 °C for 8 h. In the meantime, 0.51 g of $AgNO_3$ and 3.62 mg of NaCl were dissolved in 10 mL and 20 mL of glycerol, respectively. The NaCl solution was stirred and heated at 50 °C in order to obtain the clear solution. Then, $AgNO_3$ and NaCl were added into PVP solution and stirred for 3 min at 100 °C, the solution changed from transparent to orange which confirmed the silver nanoparticles seed growth. The mixed solution was instantly transferred to the Teflon-lined stainless-steel autoclave and heat at 150 °C for 5.5 h for the growing of AgNW. The AgNW was purified by washing with the mixed solvent between deionized water and absolute ethanol (ratio 1:1) several times and centrifuged at 4500 rpm for 10 min. Finally, AgNW was washing with ethanol 3 more times and re-dispersed in ethanol for further used.

2.3. PEM fabrication

PEM were fabricated on a glass substrate which was sequentially sonicated in DI water, acetone, isopropanol, and dried with Argon. The glass slides were then treated under UV light for 15 min and sequentially immersed for 1 min into a 10 mM solution of PDADMAC or PSS with 1 M NaCl. After each polyelectrolyte immersion step, the excess PDADMAC or PSS was removed by rinsing the sample in DI water 30 s, 3 times. This dipping cycle was repeated until the number of desired layer was reached and dried with a stream of Argon. Three different types of sample were prepared before spin coating that were plain glass slide, glass slide with 7 layers of PDADMAC-PSS, positive on top, and glass slide with 8 layers of PDADMAC-PSS, negative on top. The AgNW monolayer were deposited on the samples by spin coating at 1000 rpm for 1 min as described in Fig. 1. The 1000 rpm of rotation speed was chosen as it provided the most uniform coatings on the samples (Data not shown). The substrates were next post-annealed at 150 °C for 10 min in order to dry the films and improve the electrical properties of AgNW network on the substrates.

2.4. Characterization

UV-Visible spectroscopy (Jasco, V-670 spectrometer with FLH-740 head) was used to observe the optical properties of AgNW and also the transparency which was measured at 550 nm. X-Ray diffraction spectroscopy (XRD, Rigaku SmartLab, Japan) was used to record the X-ray diffraction pattern of AgNW using Cu Kα radiation at room temperature with scan rate of $2\theta = 2°$/min and scanning from 30 to 90°. Field emission scanning electron microscope (FESEM, S-4800, Hitachi) was used to observe the size, shape and morphology of AgNW on the specimen's surface. The peeling resistance was observed by using the captain scotch tape (927AR grade) with thickness of 0.055 mm. Atomic force microscopy (AFM, Park system XE-Series, non-contact mode) was used to observe the surface topology of the AgNW on the substrate. The sheet resistance was measured with a 4 point probe setup (Lucas labs model 302) connected to a Keithley 236 source measure unit. The distance between each probe was 0.5 mm. The glass specimen was cut to 2 cm × 2.5 cm and coated with PEM followed by AgNW deposition via spin coating.

3. Result and discussion

The AgNW were synthesized using the solvothermal process with

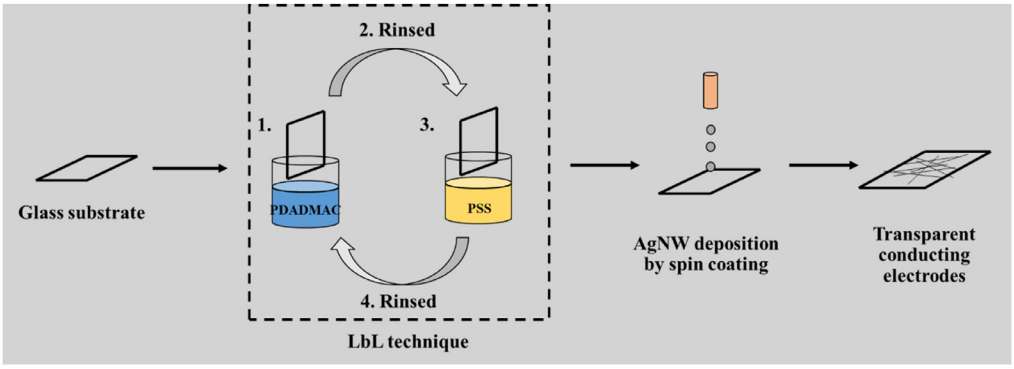

Fig. 1. Schematic of the method used for the AgNW deposition on glass slides modified with 0, 7 and 8 layers of PDADMAC-PSS.

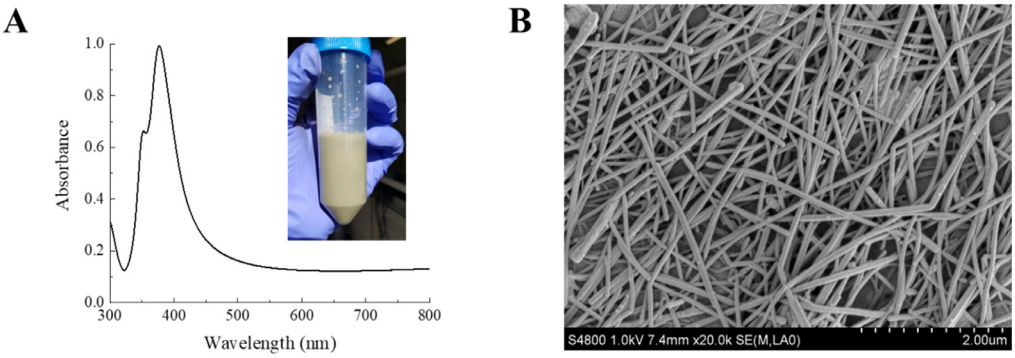

Fig. 2. UV–Vis absorption spectra and pictures of the AgNW solution (A) and FESEM image of AgNW (B).

PVP and glycerol as stabilizer and reducing agent. The synthesis was carried out with NaCl in solution leading to the formation of silver chloride complex which was later reduced to silver Ag^0 and obtained uniform and long AgNW. Although, ethylene glycol is a common reducing agent in the synthesis of AgNW, glycerol was used here as an alternative reducing agent. Glycerol has a higher boiling point (290 °C) and a higher hydroxyl group content than ethylene glycol which accelerated the wires growth [27,45]. As in other published work, PVP was used to control the growth direction of AgNW as it present favorable adsorption onto the (100) face of the multiple-twined particle of silver. This preferential adsorption leaves the (111) face unprotected, thus inducing a longitudinal growth of the wire perpendicular to the (111) direction. A monolayer of AgNW was then spin-coated on the PEM primer which acted as the adhesive layer as described earlier. The PEM top layer is expected to provide an anchoring site for the AgNW and possibly to enhance the peeling resistivity and also the AgNW packing density on the substrate when compared to deposition on bare glass surface. Electron microscopy was used to observe the morphology of the wire which should display nanometer scale diameter but micron scale length. On the FESEM images of AgNW shown in Fig. 2, it can be seen that the diameter of the AgNW is between 20 and 30 nm with a length ranging from 10 to 30 μm confirming the synthesis of the silver nanowires. Typically, spherical silver nanoparticles usually display an absorbance peak centered around 400 nm, depending on size, shape and surrounding media. This plasmonic peak is due to the collective oscillation of the delocalized free electron in the metallic nanoparticle under electro-magnetic excitation. From the UV absorption spectrum of AgNW, two peaks are usually observed in the literature [28] at 350 and 380 nm, which are characteristic of the AgNW UV–Vis spectra. In Fig. 2, these two peaks are clearly visible and no peak can be seen after 400 nm suggesting that all the silver nanoparticles have been consumed and transformed to silver wires. If the silver nanoparticles were only converted to short silver rods having small aspect ratio (10–50), they would present a longitudinal resonance plasmon peak shifted to higher wavelength in the visible range. Here, the wires with an aspect ratio of nearly 1000 only display transverse plasmon band and their secondary peak is not visible. Both UV absorption spectra and FESEM image confirm that no silver nanoparticle seed are left after completion of the reaction and that the AgNW with a diameter of 20–30 nm and a length of around 20–30 μm have been synthesized.

The crystal structure of the AgNW was studied by X-Ray Diffraction pattern analysis. As the wires grow in the (111) plane direction, this lattice should be dominant in the asymmetric growth of the silver crystal. The XRD analysis of the sample shown in Fig. 3 display the characteristic diffraction pattern of the face centered cubic of AgNW which consists of two main diffraction peaks at 38.3° and 44.7°. These two largely predominant peaks that correspond to the (111) and (200) diffraction planes hinder the observation of the (220) and (311) that should appear at 64.9° and 78.1°, as suggested by Shobin et al. [28,46].

It was initially hypothesized that the PEM coatings could enhance

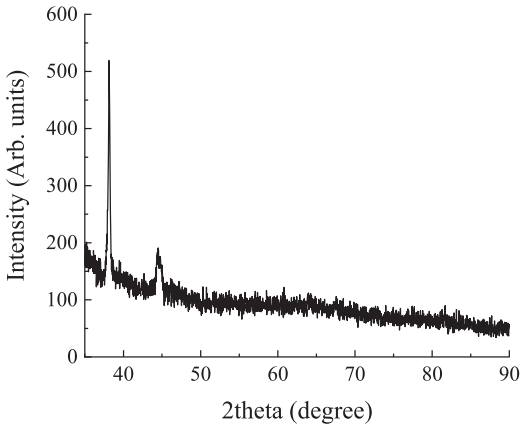

Fig. 3. Plot of the XRD pattern from a thin film of AgNW coated on a glass substrate.

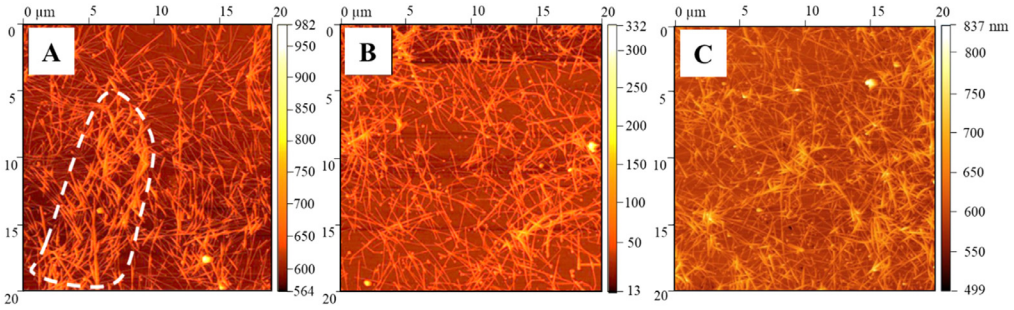

Fig. 4. AFM images of the AgNW coated on (A) bare glass, (B) glass slide with 8 PDADMAC-PSS layers and (C) glass slide with 7 PDADMAC-PSS layers.

the deposition and stability of AgNW on glass slides. To test this hypothesis, a PEM primer layer was deposited on glass slides with 7 or 8 layers to provide either a cationic or anionic top surface charge. PVP is a non-ionic polymer used to stabilize the AgNW and its possible interaction with the PEM was tested on both charge surfaces. The number of layers studied was selected to be 7 and 8 in order to investigate the effect of the top layer's electrostatic charge toward peeling resistance. Preliminary results confirmed that when a lower number of PDADMAC and PSS layer were used (1–6 layers), the AgNW were unstable probably due to incomplete coverage of the surface by the PEM primer. It is well known that PEM coatings requires several layers in order to achieve homogenous coverage of the substrates [47]. Further increase of the number of layers did not lead to any improvement in the AgNW stability so 7 and 8 layers were used in this study. Therefore, AgNW were deposited by spin coating on bare glass slide and glass slides coated with 7 or 8 layers of PEM. The surface of the samples after spin coating was analyzed using AFM to study their topology and surface roughness (Fig. 4).

From the AFM images of all the samples, it can be seen that the AgNW are individually deposited and no aggregation of single AgNW into bundles is observable. The diameter measured using the AFM by cross section analysis confirm a diameter of 20–30 nm which is consistent with the FESEM images in Fig. 2. It can be seen that the AgNW deposited on the glass substrate (Fig. 4A) appear partially aggregated into clusters, suggesting a less uniform coating with an average roughness of 28.87 nm. The aggregation of the wires is probably due to the residual mobility of the wires during solvent evaporation due to poor AgNW-glass interaction. The anionic PEM 8 layers coated with the AgNW displayed a more homogeneous dispersion due to the better anchoring, but the wires density appear lower which might be due to the repulsive force between anionic PSS and carbonyl groups found on the PVP capping. Interestingly, the cationic PEM 7 layers displayed a more homogeneous and higher density coating as seen in Fig. 4C. The surface roughness of AgNW on PEM 7 and 8 layers were measured to be 28.02 and 23.9 nm, respectively. This increase in roughness could be a problem when using the AgNW as transparent electrodes in solar cells because the roughness can lead to the creation of a short circuit between the different active layers. A possible solution to this problem is to add ZnO nanoparticles by spin coating onto the AgNW layers. The ZnO are often used in solar cell application and could have a double role here. Firstly, they can fill the gap between the AgNW thus reducing the surface roughness. Secondly, they can act as a hole-blocking layer and improve the charge separation efficiency.

The AgNW coating density can also be evaluated by using UV–Vis spectroscopy, which is proportional to the AgNW local density. In Fig. 5, the absorbance values for each coating are compiled and it can be seen that PEM 7 layers coating has a higher absorbance at 350 and 380 nm when compared to PEM 8 layers and bare glass slide, thus confirming AFM images.

With transparency, the other most critical characteristic of the AgNW coating is its electrical conductivity. In Fig. 6, the sheet resistance of samples prepared from increasing AgNW content and spin-

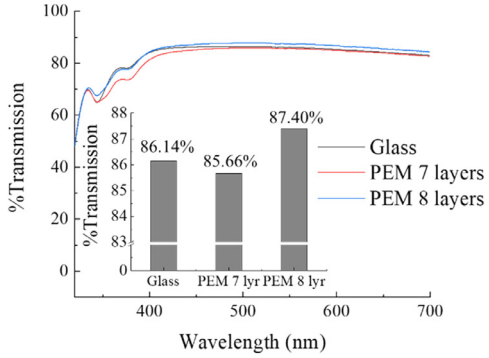

Fig. 5. UV–Vis transmission spectra of the AgNW (0.7% w/v) coated on glass and 7 or 8 layers of PEM. The inset represents the %transmission values at 550 nm for each sample.

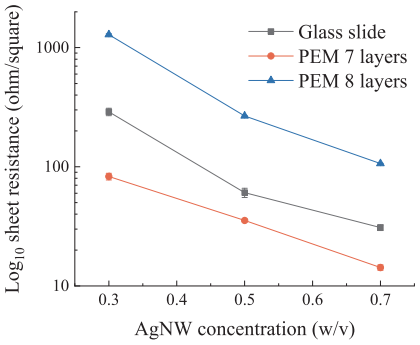

Fig. 6. Plot of the log of sheet resistance of the AgNW coating on bare glass, 7 and 8 layers PDADMAC-PSS layers as a function of the concentration of AgNW (w/v) in solution.

coated on bare glass slides and PEM 7 or 8 layers is shown. Using the 4-points probe technique to evaluate the conducting properties of the different coating, the sheet resistances of the AgNW (0.7 %wt.) coated on glass and PEM 8 layers were measured to be 30 and 106 Ω/square, respectively (Fig. 6). The AgNW coated on PEM 7 layers had sheet resistance as low as 14 Ω/square. It can also be seen that the sheet resistance decreased with the increasing AgNW concentration which is fairly intuitive. Nevertheless, the 7 layers coating produced a denser and more homogeneous AgNW coating with the best conductivity when compared to blank and 8 layers coating. Although, AgNW and PVP do not carry a clear anionic charge, favorable interaction between the lone pair on the N and PDADMAC coating are expected. Similar affinity between N atom in PAH and the AgNW have previously been reported by Kim et al. [40]. They used XPS was used to confirm the formation of coordinating bond between the nitrogen atom and the AgNW surface. The superior attachment between the 7th layer and the AgNW is also probably due to the favorable interactions between the quaternary amine N^+ and the nucleophile carbonyl found on the pyrrolidone

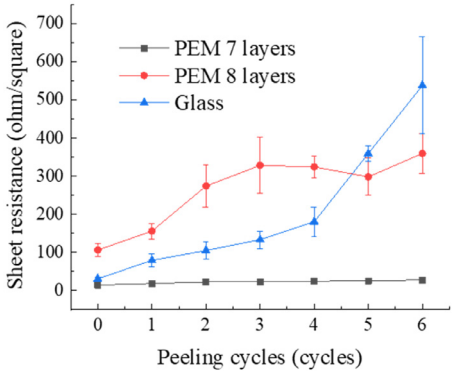

Fig. 7. Plot of the sheet resistance of the AgNW coated on glass, PEM 7 and 8 layers as a function of the number of peeling cycles.

pendant groups used to stabilize the AgNW. In contrast the 8th layer being highly negative due to the presence of sulfonic groups of PSS, probably lead to very poor bonding with the PVP which leads to a poor peeling resistance in the following paragraphs. On the other hand, both glass and PEM 8 layers substrate display higher sheet resistance suggesting aggregation and poor coating density. Although all samples could be coated by spin coating with more or less success, it is necessary to investigate the stability of the wire on the surface with a peeling test 6 cycles of pressing a scotch tape strip on different samples followed by quick peeling.

As displayed in Fig. 7, the sheet resistance of AgNW coating was measured after each cycle and was found to increase in the case of the glass coating and PEM 8 layers from 30 to about 500 Ω/square after 6 peeling cycles suggesting poor adhesion of both coating. In contrast, the AgNW coated on the PDADMAC (PEM 7 layers) displayed a much better adhesion and stability and maintained a sheet resistance value under 25 Ω/square even after 6 cycles of peeling. It can be clearly concluded that favorable interaction between the wires and the PDADMAC layers lead to a better adhesion properties using the PEM 7 layers. As the ultimate goal is to produce flexible transparent conducting electrode, a bare PET sample was used as substrate while two other PET samples were modified with 7 and 8 layer of PDADMAC-PSS which were used as adhesive layer for AgNW. The sheet resistance of all samples after coating with AgNW were measured and plotted in Table 2.

Results show that the sheet resistance of the AgNW on PET is initially much higher than on glass (30 Ω/square for glass and 3600 Ω/square for PET) due to the hydrophobic characteristic of PET which affect to the binding of the AgNW and also the fabrication of PEM. By using the PEM 7 and 8 layers as adhesive layer, the PET surface became more hydrophilic which provided a better deposition of AgNW result in the lower sheet resistance. Similarly, to the deposition of AgNW on the glass substrate, the PEM 7 layers exhibited a better adhesion of AgNW than the PEM 8 layers while maintaining a good transparency when compared to the plain PET without AgNW. Since the application of the electrode proposed here is to be used as flexible electrode, a last test to confirm the stability of the AgNW on the 7 layers PEM was to perform a 1000 bending cycles and measure the sheet resistance every 100 cycles.

Table 2
Values of the Sheet resistance of AgNW deposited on PET or glass as a function of the number of primer layers. (Plain substrate, PEM 7 or 8 layers).

Substrate	Sheet resistance (Ω/square)	
	PET	Glass
Plain substrate	3621.32 ± 1151.61	30.86 ± 3.06
PEM 7 layers	74.30 ± 8.86	14.27 ± 1.34
PEM 8 layers	147.39 ± 11.36	106.41 ± 16.24

*The results were averaged from 5 samples at the same positions.

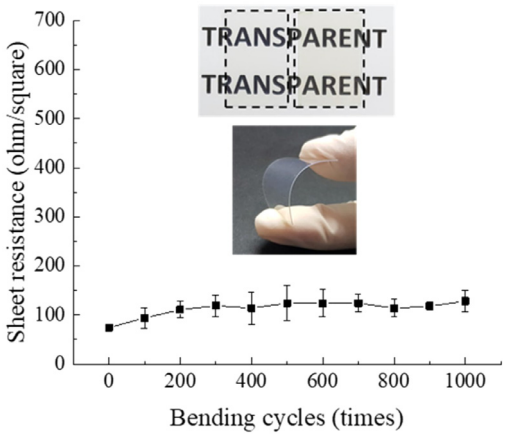

Fig. 8. Plot of sheet resistance of PET coated with AgNW as a function of bending cycle from 0 to 1000 cycles with the inset pictures of the bare and 7 layers coated PET coated (upper picture) and 7 layers coated PET (lower picture).

Results show that the sheet resistance is very stable and only increased from 74 to 128 Ω/square which confirm that the wires were strongly anchored on the 7 layers PEM (Fig. 8.).

4. Conclusion

In this work, transparent conducting electrodes were prepared by the deposition of AgNW on PEM modified glass substrates via spin coating. Although the spin coating of the AgNW on all three surfaces (bare glass slide, 7 and 8 layer of PDADMAC-PSS primer) was achieved, results show that a better anchoring of the AgNW was obtained when PDADMAC was used as top layer (7 layers) prior to spin coating in term of AgNW coating density, homogeneity and peeling resistance even after 6 peeling cycles. PET was also used as substrate for the deposition of AgNW in order to produce the flexible transparent conducting electrode which could be used in solar cell application. Results suggest that the treatment of the PET substrates, using a PEM primer with PDADMAC on top is a promising method to stabilize AgNW toward the development of robust transparent conducting electrodes for the development of optoelectronic devices.

CRediT authorship contribution statement

Jedsada Chavalitkul: Investigation, Visualization, Writing - review & editing. **Olivier Margeat:** Funding acquisition, Supervision, Writing - review & editing. **Jörg Ackermann:** Funding acquisition, Supervision, Writing - review & editing. **Stephan T. Dubas:** Funding acquisition, Supervision, Writing - original draft, Writing - review & editing.

Declaration of Competing Interest

The authors declare that they have no known competing financial interests or personal relationships that could have appeared to influence the work reported in this paper.

Acknowledgement

This work was supported by the Thailand research fund [PHD59I0034, 2015]; and Centre interdisciplinaire de nanoscience de Marseille, CINaM, Marseille.

Supplementary materials

Supplementary material associated with this article can be found, in

the online version, at doi:10.1016/j.tsf.2020.138272.

References

[1] T.-B. Song, N. Li, Emerging transparent conducting electrodes for organic light emitting diodes, Electronics (Basel) 3 (2014) 190–204.
[2] A. Kumar, Predicting efficiency of solar cell based on transparent conducting electrode, J. Appl. Phys. 121 (2017) 014502.
[3] R. Peng, W. Song, T. Yan, B. Fanady, Y. Li, Q. Zhan, Z. Ge, Interface bonding engineering of a transparent conductive electrode towards highly efficient and mechanically flexible ITO-free organic solar cells, J. Mater. Chem. A 7 (2019) 11460–11467.
[4] J. Meiss, M.K. Riede, K. Leo, Towards efficient tin-doped indium oxide (ITO)-free inverted organic solar cells using metal cathodes, Appl. Phys. Lett. 94 (2009) 013303.
[5] H. Makino, N. Yamamoto, A. Miyake, T. Yamada, H. Iwaoka, P-7: Ga-Doped ZnO transparent conductive film as substitution for ITO common electrode in TFT-LCDs, SID Symposium DIgest of Technical Papers, 40 2009, pp. 1103–1106.
[6] N.M. Bedford, M.B. Dickerson, L.F. Drummy, H. Koerner, K.M. Singh, M.C. Vasudev, M.F. Durstock, R.R. Naik, A.J. Steckl, Nanofiber-based bulk-heterojunction organic solar cells using coaxial electrospinning, Adv. Energy Mater. 2 (2012) 1136–1144.
[7] T.-H. Han, S.-H. Jeong, Y. Lee, H.-K. Seo, S.-J. Kwon, M.-H. Park, T.-W. Lee, Flexible transparent electrodes for organic light-emitting diodes, J. Inf. Display 16 (2015) 71–84.
[8] S.W. Shin, Y.U. Jung, K.-B. Kim, S.-W. Choi, S.J. Kang, ITO-free transparent conductive films based on carbon nanomaterials with metal grid for liquid crystal displays, Liq. Cryst. 42 (2015) 954–958.
[9] D. Kim, L. Zhu, D.-J. Jeong, K. Chun, Y.-Y. Bang, S.-R. Kim, J.-H. Kim, S.-K. Oh, Transparent flexible heater based on hybrid of carbon nanotubes and silver nanowires, Carbon 63 (2013) 530–536.
[10] K. Sakamoto, H. Kuwae, N. Kobayashi, A. Nobori, S. Shoji, J. Mizuno, Highly flexible transparent electrodes based on mesh-patterned rigid indium tin oxide, Sci. Rep. 8 (2018) 2825.
[11] P.C. Hsu, S. Wang, H. Wu, V.K. Narasimhan, D. Kong, H. Ryoung Lee, Y. Cui, Performance enhancement of metal nanowire transparent conducting electrodes by mesoscale metal wires, Nat. Commun. 4 (2013) 2522.
[12] M. Arefpour, M. Almasi Kashi, F. Khansari Barzoki, M. Noormohammadi, A. Ramazani, Electrodeposited metal nanowires as transparent conductive electrodes: their release conditions, electrical conductivity, optical transparency and chemical stability, Mater. Des. 157 (2018) 326–336.
[13] C.F. Guo, Z. Ren, Flexible transparent conductors based on metal nanowire networks, Mater. Today 18 (2015) 143–154.
[14] R. Zhang, M. Engholm, Recent progress on the fabrication and properties of silver nanowire-based transparent electrodes, Nanomaterials (Basel 8 (2018) 628.
[15] Z.C.Z. Wu, X. Du, J.M. Logan, J. Sippel, M. Nikolou, K. Kamaras, J.R. Reynolds, D.B. Tanner, A.F. Hebard, A.G. Rinzler, Transparent, conductive carbon nanotube films, Science 205 (2004) 1273–1276.
[16] O. Urper, İ. Çakmak, N. Karatepe, Fabrication of carbon nanotube transparent conductive films by vacuum filtration method, Mater. Lett. 223 (2018) 210–214.
[17] Y.S. Woo, Transparent conductive electrodes based on graphene-related materials, Micromach. (Basel 10 (2018) 13.
[18] C. Guillén, J. Herrero, Transparent conductive ITO/Ag/ITO multilayer electrodes deposited by sputtering at room temperature, Opt. Commun. 282 (2009) 574–578.
[19] G. Zeng, J. Zhang, X. Chen, H. Gu, Y. Li, Y. Li, Breaking 12% efficiency in flexible organic solar cells by using a composite electrode, Sci. China Chem. 62 (2019) 851–858.
[20] L. Mao, Q. Chen, Y. Li, Y. Li, J. Cai, W. Su, S. Bai, Y. Jin, C.-Q. Ma, Z. Cui, L. Chen, Flexible silver grid/PEDOT:PSS hybrid electrodes for large area inverted polymer solar cells, Nano Energy 10 (2014) 259–267.
[21] A.H. Alami, B. Rajab, K. Aokal, Assessment of silver nanowires infused with zinc oxide as a transparent electrode for dye-sensitized solar cell applications, Energy 139 (2017) 1231–1236.
[22] M. Singh, P. Prasher, J. Kim, Solution processed silver-nanowire/zinc oxide based transparent conductive electrode for efficient photovoltaic performance, Nano-Struct. Nano-Obj. 16 (2018) 151–155.
[23] M. Chalh, S. Vedraine, B. Lucas, B. Ratier, Plasmonic Ag nanowire network embedded in zinc oxide nanoparticles for inverted organic solar cells electrode, Sol. Energy Mater. Sol. Cells 152 (2016) 34–41.
[24] X. Chen, G. Xu, G. Zeng, H. Gu, H. Chen, H. Xu, H. Yao, Y. Li, J. Hou, Y. Li, Realizing ultrahigh mechanical flexibility and >15% efficiency of flexible organic solar cells via a “welding” flexible transparent electrode, Adv. Mater. 32 (2020) e1908478.
[25] T. Tokuno, M. Nogi, M. Karakawa, J. Jiu, T.T. Nge, Y. Aso, K. Suganuma, Fabrication of silver nanowire transparent electrodes at room temperature, Nano Res. 4 (2011) 1215–1222.
[26] P. Zhang, I. Wyman, J. Hu, S. Lin, Z. Zhong, Y. Tu, Z. Huang, Y. Wei, Silver nanowires: synthesis technologies, growth mechanism and multifunctional applications, Mater. Sci. Eng. B 223 (2017) 1–23.
[27] B. Liu, H. Yan, S. Chen, Y. Guan, G. Wu, R. Jin, L. Li, Stable and controllable synthesis of silver nanowires for transparent conducting film, Nanoscale Res. Lett. 12 (2017) 212.
[28] S. Coskun, B. Aksoy, H.E. Unalan, Polyol synthesis of silver nanowires: an extensive parametric study, Cryst. Growth Des. 11 (2011) 4963–4969.
[29] Y. Ran, W. He, K. Wang, S. Ji, C. Ye, A one-step route to Ag nanowires with a diameter below 40nm and an aspect ratio above 1000, Chem. Commun. (Camb.) 50 (2014) 14877–14880.
[30] H.-W. Jang, B.-Y. Hwang, K.-W. Lee, Y.-M. Kim, J.-Y. Kim, Controlling the size of silver nanowires produced by a tetrabutylammonium dichlorobromide salt-based polyol process: kinetics of silver crystal growth, AIP Adv. 8 (2018) 025303.
[31] H. Wang, Y. Wang, X. Chen, Synthesis of uniform silver nanowires from AgCl seeds for transparent conductive films via spin-coating at variable spin-speed, Colloids Surf. A 565 (2019) 154–161.
[32] Y. Ko, J. Kim, D. Kim, Y. Yamauchi, J.H. Kim, J. You, A simple silver nanowire patterning method based on poly(ethylene glycol) photolithography and its application for soft electronics, Sci. Rep. 7 (2017) 2282.
[33] H. Yun, D. Seo, M. Lee, S. Kwon, L. Park, Effective synthesis and recovery of silver nanowires prepared by tapered continuous flow reactor for flexible and transparent conducting electrode, Metals (Basel) 6 (2016).
[34] J.-Y. Lee, D. Shin, J. Park, Fabrication of silver nanowire-based stretchable electrodes using spray coating, Thin Solid Films 608 (2016) 34–43.
[35] F. Selzer, N. Weiss, D. Kneppe, L. Bormann, C. Sachse, N. Gaponik, A. Eychmuller, K. Leo, L. Muller-Meskamp, A spray-coating process for highly conductive silver nanowire networks as the transparent top-electrode for small molecule organic photovoltaics, Nanoscale 7 (2015) 2777–2783.
[36] J.S. Woo, G.-W. Lee, S.-Y. Park, J.T. Han, Realization of transparent conducting networks with high uniformity by spray deposition on flexible substrates, Thin Solid Films 638 (2017) 367–374.
[37] C. Sachse, L. Müller-Meskamp, L. Bormann, Y.H. Kim, F. Lehnert, A. Philipp, B. Beyer, K. Leo, Transparent, dip-coated silver nanowire electrodes for small molecule organic solar cells, Org. Electron. 14 (2013) 143–148.
[38] T.K. Junaidi, S.E. Harsojo, High-performance silver nanowire film on flexible substrate prepared by meyer-rod coating, Mater. Sci. Eng. B 202 (2017).
[39] S. Zhang, X. Liu, T. Lin, P. He, A method to fabricate uniform silver nanowires transparent electrode using Meyer rod coating and dynamic heating, J. Mater. Sci. Mater. Electron. 30 (2019) 18702–18709.
[40] C. Kim, H. An, A. Jung, B. Yeom, Vortex-assisted layer-by-layer assembly of silver nanowire thin films for flexible and transparent conductive electrodes, J. Colloid Interface Sci. 493 (2017) 371–377.
[41] B. Wei, X. Wu, L. Lian, S. Yang, D. Dong, D. Feng, G. He, A highly conductive and smooth AgNW/PEDOT:PSS film treated by hot-pressing as electrode for organic light emitting diode, Org. Electron. 43 (2017) 182–188.
[42] S.T. Dubas, J.B. Schlenoff, Factors controlling the growth of polyelectrolyte multilayers, Macromolecules 32 (1999) 8153–8160.
[43] S.T. Dubas, J.B. Schlenoff, Swelling and smoothing of polyelectrolyte multilayers by salt, Langmuir 17 (2001) 7725–7727.
[44] Y. Li, S. Guo, H. Yang, Y. Chao, S. Jiang, C. Wang, One-step synthesis of ultra-long silver nanowires of over 100μm and their application in flexible transparent conductive films, RSC Adv. 8 (2018) 8057–8063.
[45] C. Yang, Y. Tang, Z. Su, Z. Zhang, C. Fang, Preparation of silver nanowires via a rapid, scalable and green pathway, J. Mater. Sci. Technol. 31 (2014) 16–22.
[46] L.R. Shobin, S. Manivannan, One pot rapid synthesis of silver nanowires using NaCl assisted glycerol mediated polyol process, Electron. Mater. Lett. 10 (2014) 1027–1031.
[47] J.B. Schlenoff, S.T. Dubas, Mechanism of polyelectrolyte multilayer growth: charge overcompensation and distribution, Macromolecules 34 (2001) 592–598.